Glass physics

- > Introduction
- > Systems
- > Structure
- > Glass transition
- > MCT
- > Metallic glasses
- > Mechanical properties
- > Applications

Hermann Franz
Master course Modern X-ray Physics
12 May 2011

Introduction

Glasses are materials with "amorphous structure showing a gradual transition from the liquid to the solid without well defined melting point."

- Favorable conditions for forming
- Particular mechanical properties

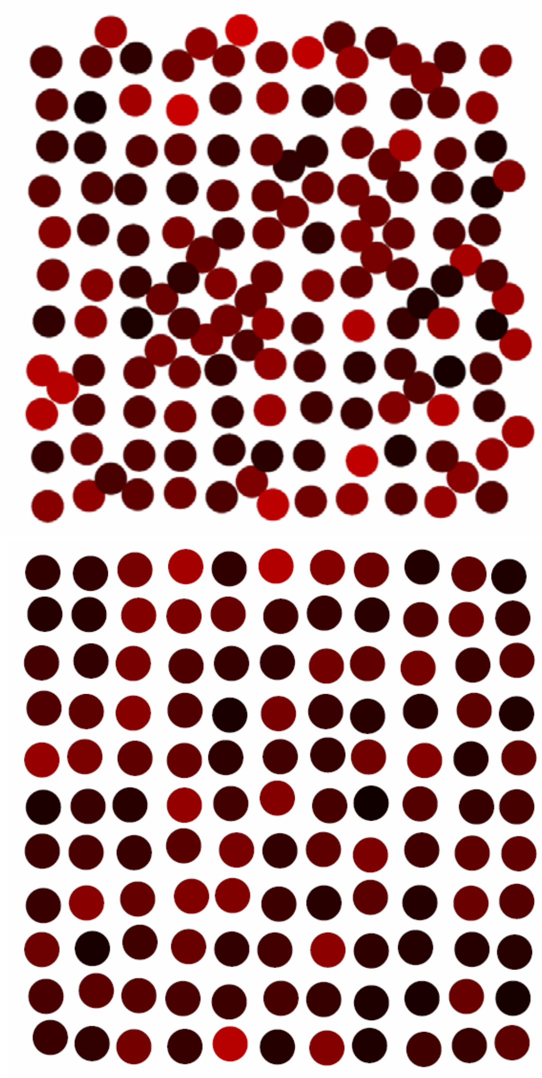

Introduction

Physical properties change gradually on lowering the temperature

Cross-over depends on cooling/heating rate

i.e. properties depend on thermal history

Glasses are in a frozen in meta-stable state

► susceptible to crystallization

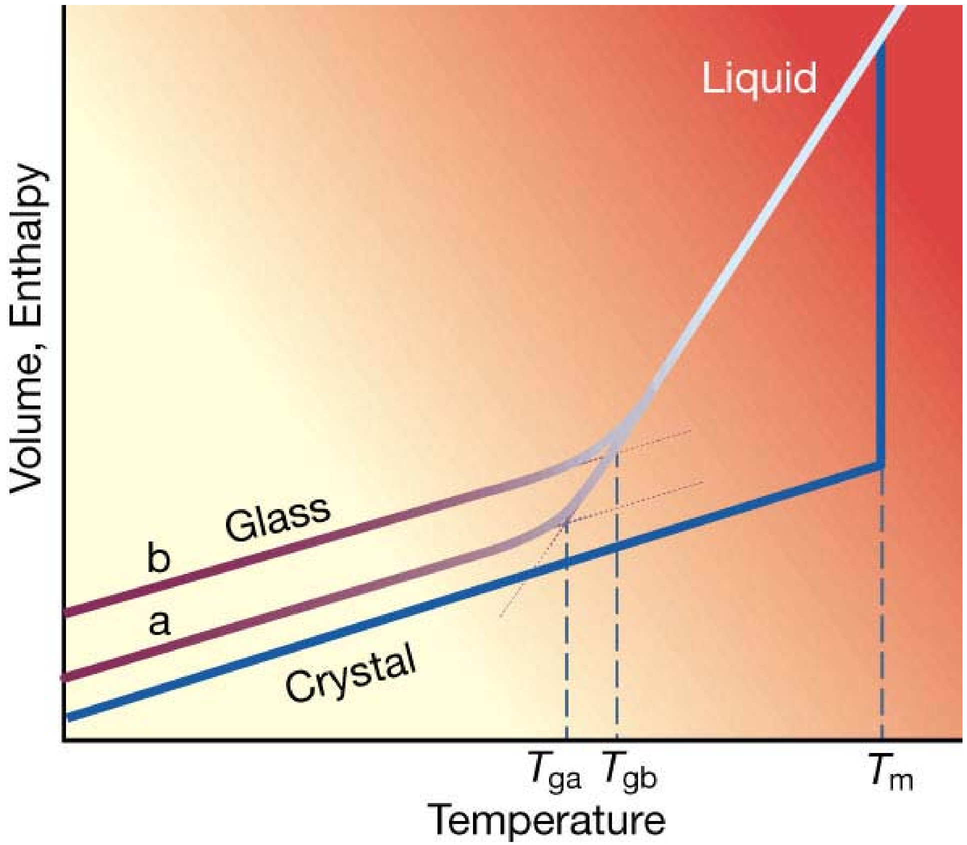

Examples for glasses in everyday life

Traditional glasses

SiO_2, B_2O_3, P_2O_5 based

Window glass

SiO_2 with sodium or potassium

minerals (soda, potash)

Glasses for art work

doped with variety

of elements

Industrial glasses

Polymers

Plastic materials: PE, PMMA, PS…..

SMO (small organic molecules)

Glycerol, OTP, salol, squalane, ……

Metallic glasses

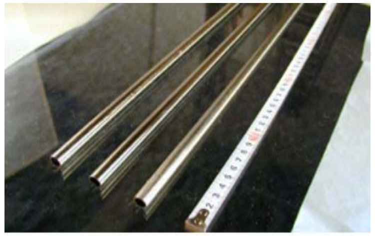

History

Art of glass making known since

ca 3000 b.c.

Earliest records in Egypt and Mesopotamia, later many records in Rome

Sacophagus of Tut Ench Amun

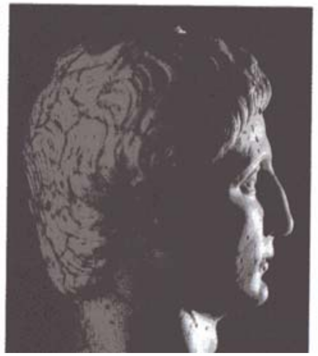

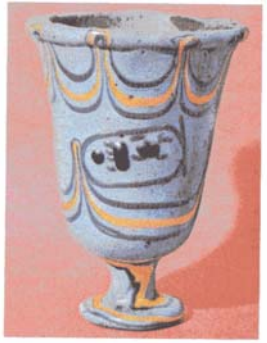

Glas 2): Becher aus dem Grab Thutmosis' III.; Höhe 8,5 cm, um 1450 v. Chr. (München, Staatliche Sammlung Ägyptischer Kunst)

Structure by X-rays

Reminder:

Scattering amplitude from a crystal

$$F^{crystal}(Q) = \underbrace{\sum_{rj} F_j^{mol}(Q)\exp(i\mathbf{Qr}_j)}_{\text{unit cell structure factor}} \bullet \underbrace{\sum_{Rn} \exp(i\mathbf{QR}_n)}_{\text{lattice sum}}$$

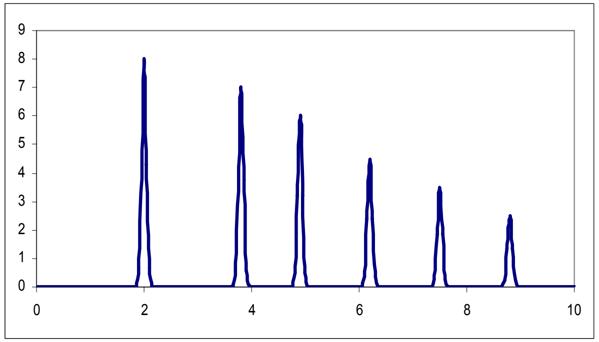

leading to reciprocal lattice

$$\mathbf{G}\bullet\mathbf{R}_n = 2\pi\,(hn_1 + kn_2 + ln_3)$$

As there is no lattice in amorphous structures we have to treat the whole sample like a molecule

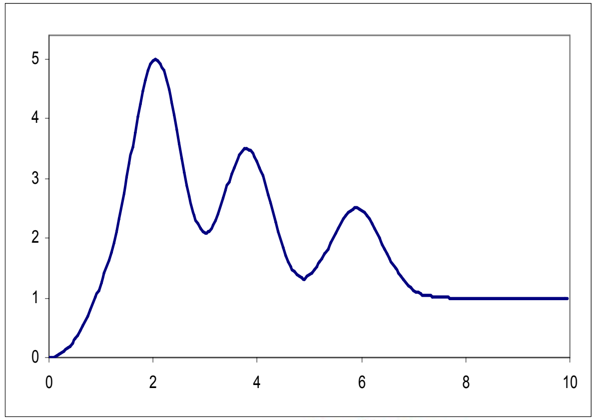

$$F^{mol}(Q) = \sum_{rj} f_j(Q)\exp(i\mathbf{Qr}_j)$$

With the sum running over all atoms in the illuminated volume

Structure by X-rays - temperature dependence

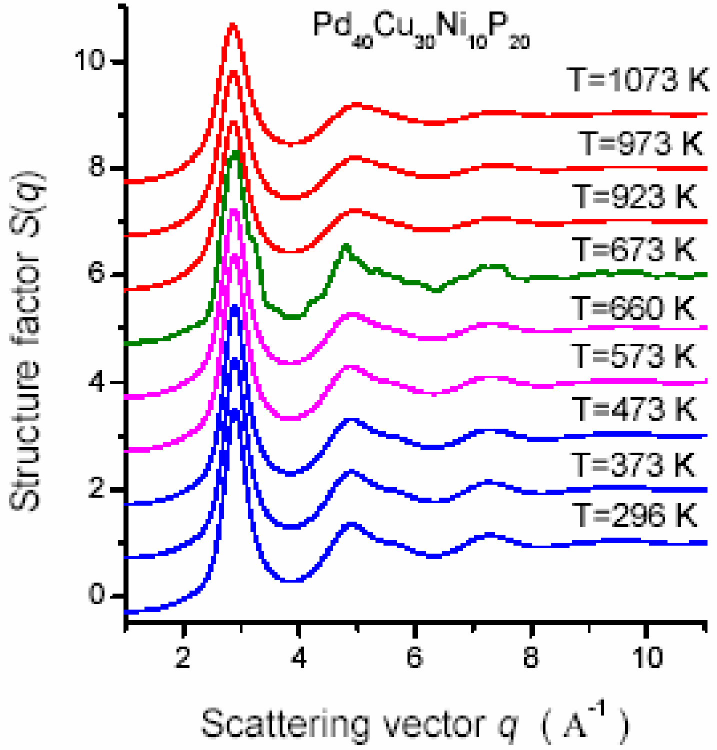

Fig.1:Structure factor $S_T(q)$ of $Pd_{40}Cu_{30}Ni_{10}P_{20}$ at different temperatures

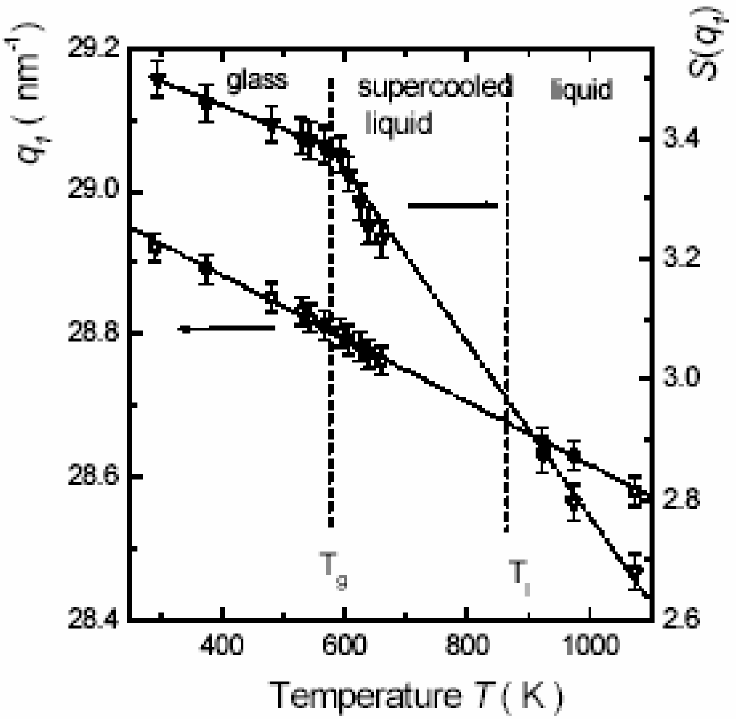

Fig.2: Position q_1 and height $S(q_1)$ of the first maximum of the structure factor $S_T(q)$ vs temperature

N. Mattern et al APL 2003

Structure determination of amorphous materials

X-ray diffraction using high energy photons

+ high penetration depths (mm-cm)
+ relatively fast, suitable for in-situ studies
- less sensitive to elements
- ASF depend on Q

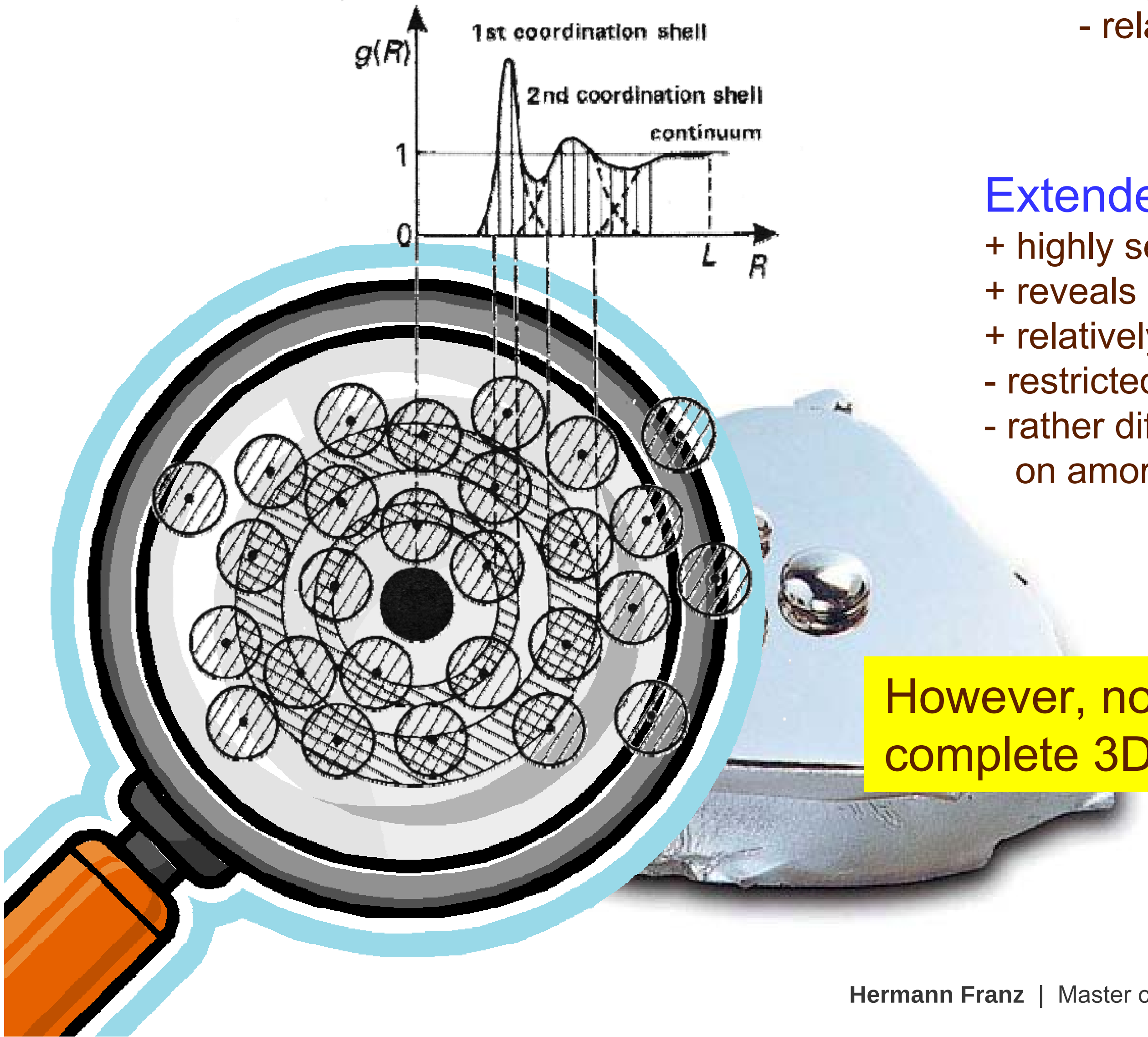

Neutron diffraction

+ sensitive to different isotopes
+ ASF do not depend on Q
+ probes magnetic state of matter
- large sample volumes
- relatively slow, not suitable for in-situ studies

Extended X-ray Absorption Spectroscopy

+ highly sensitive to elements
+ reveals local atomic configuration
+ relatively fast, suitable for in-situ studies
- restricted sample size, geometry
- rather difficult to quantitatively analyze data on amorphous samples

However, none of these techniques gives a complete 3D image of amorphous structure ☹

Reverse Monte Carlo modeling

Diffraction:

The partial $g_{ij}(r)$ functions are calculated from the atomic coordinates and transformed to reciprocal space:

$$S_{ij}(Q) = \frac{4\pi\rho c_j}{Q}\int r\sin Qr(g_{ij}(r)-1)dr$$

together with a weights (for ND $f(Q)=b$)

$$w_{ij} = \frac{(2-\delta_{ij})c_i c_j f_i(Q) f_j(Q)}{\sum_{ij} c_i c_j f_i(Q) f_j(Q)}$$

are combined in total structure factor

$$S^{RMC}(Q) = \sum_{ij} w_{ij}(Q) S_{ij}(Q)$$

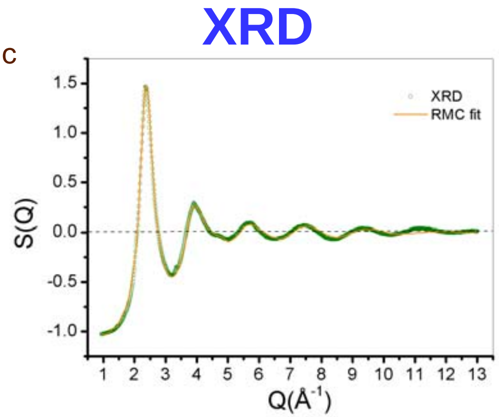

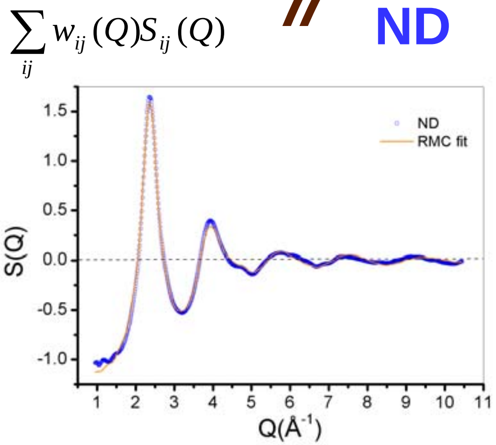

Move:

One particle is moved randomly taking into account applied constraints.

Settling:

Everything is repeated until ψ^2 begins to oscillate around a constant value.

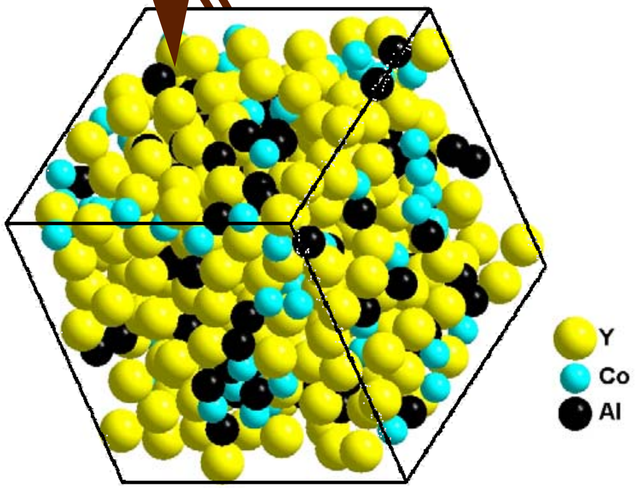

EXAFS:

The model of EXAFS signal $\chi_i(k)$, at the absorption edge of i-type atoms can be calculated from the g_{ij}:

$$\chi_i(k) = \sum_j 4\pi c_j \rho \int_0^\infty r^2 \gamma_{ij}(r,k) g_{ij}(r)dr$$

while γ_{ij} is the atomic pair backscattering signal

$$\gamma_{ij}(r,k) = A_{ij}(k,r)\sin(2kr + \Phi_{ij}(kr))$$

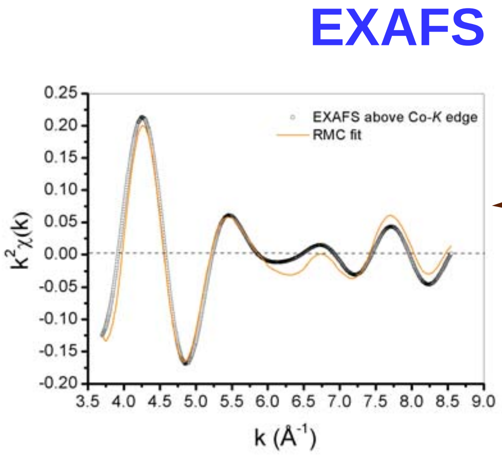

Acceptance of the move:

First the experiment-model difference is calculated

$$\psi^2 = \frac{1}{\delta}\sum_{i=1}^{m}\left[\zeta^{\exp} - \zeta^{RMC}\right]^2$$

If $\psi^2_{n+1} < \psi^2_n$ the move is always accepted.

If $\psi^2_{n+1} > \psi^2_n$ the move is accepted with the probability $\exp[-(\psi^2_{n+1} - \psi^2_n)/2]$

Courtesy of Dr. K. Saksl

RMC modeling of $Y_{56}Co_{20}Al_{24}$ bulk metallic glass

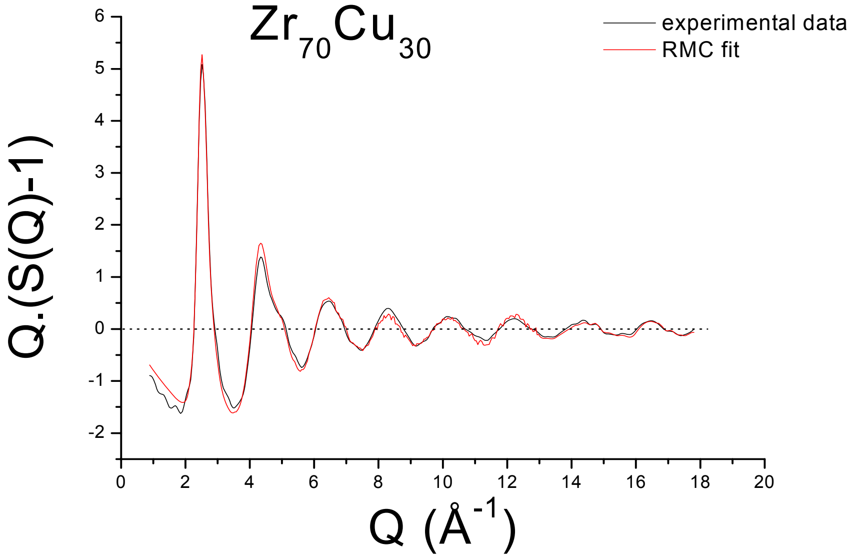
$Zr_{70}Cu_{30}$
experimental data
RMC fit
Q.(S(Q)-1)
Q (Å^{-1})
6
5
4
3
2
1
0
-1
-2
0
2
4
6
8
10
12
14
16
18
20

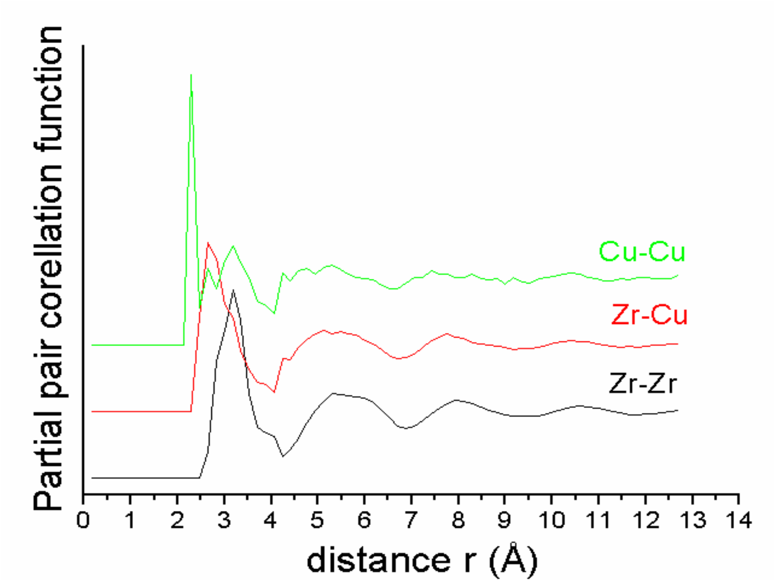
Partial pair corellation function
distance r (Å)
Cu-Cu
Zr-Cu
Zr-Zr
0
1
2
3
4
5
6
7
8
9
10
11
12
13
14

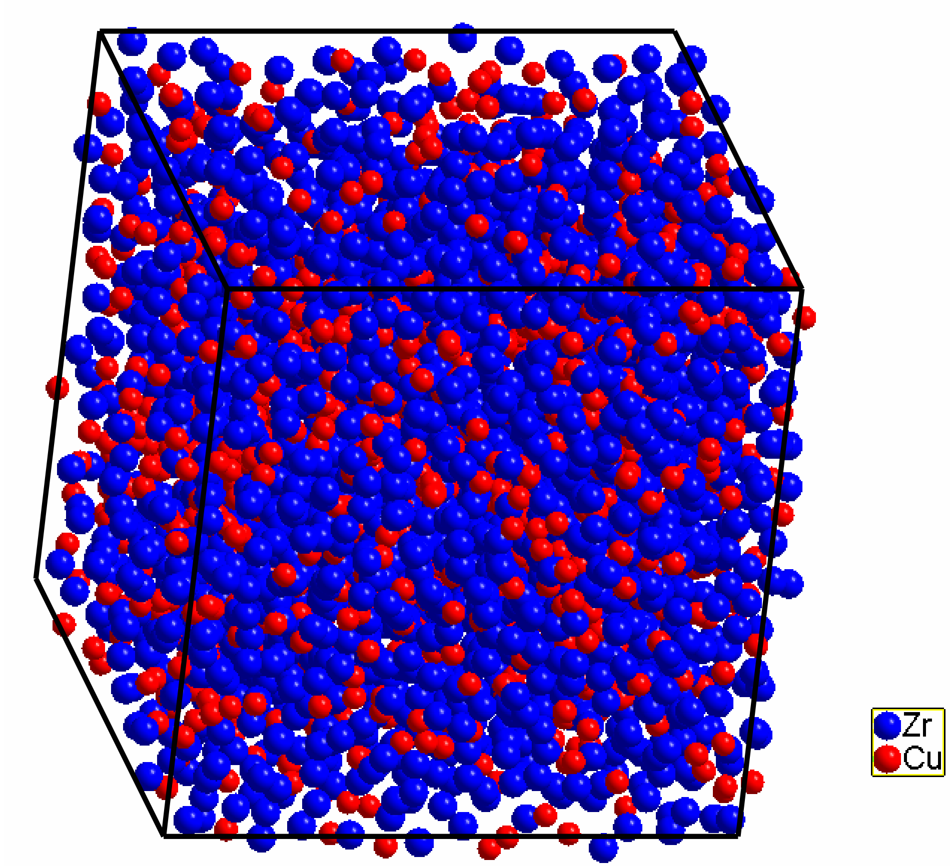
Zr
Cu

Structure by X-rays - temperature dependence II

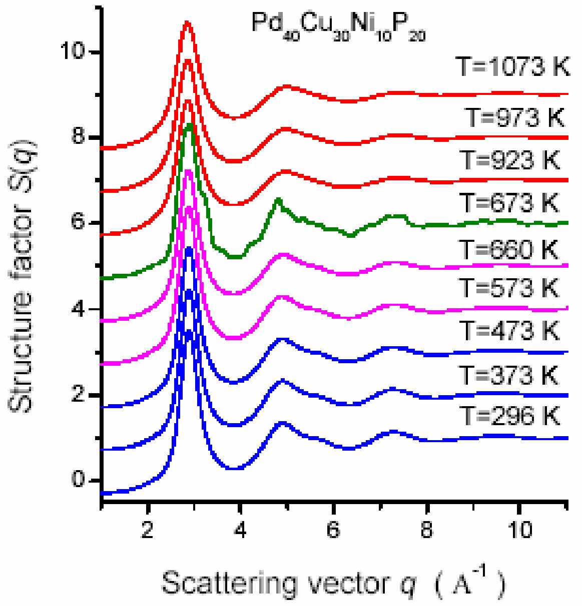

Fig.1:Structure factor $S_T(q)$ of $Pd_{40}Cu_{30}Ni_{10}P_{20}$ at different temperatures

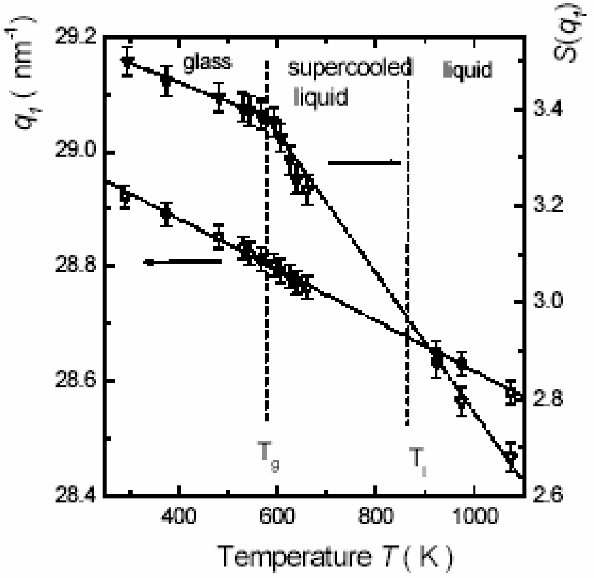

Fig.2: Position q_1 and height $S(q_1)$ of the first maximum of the structure factor $S_T(q)$ vs temperature

N. Mattern et al

APL 2003

Below T_g: harmonic change, described by Debye behavior

At T_g: Transition to lower Debye-temperature

+ structural changes

The glass transition temperature T_g

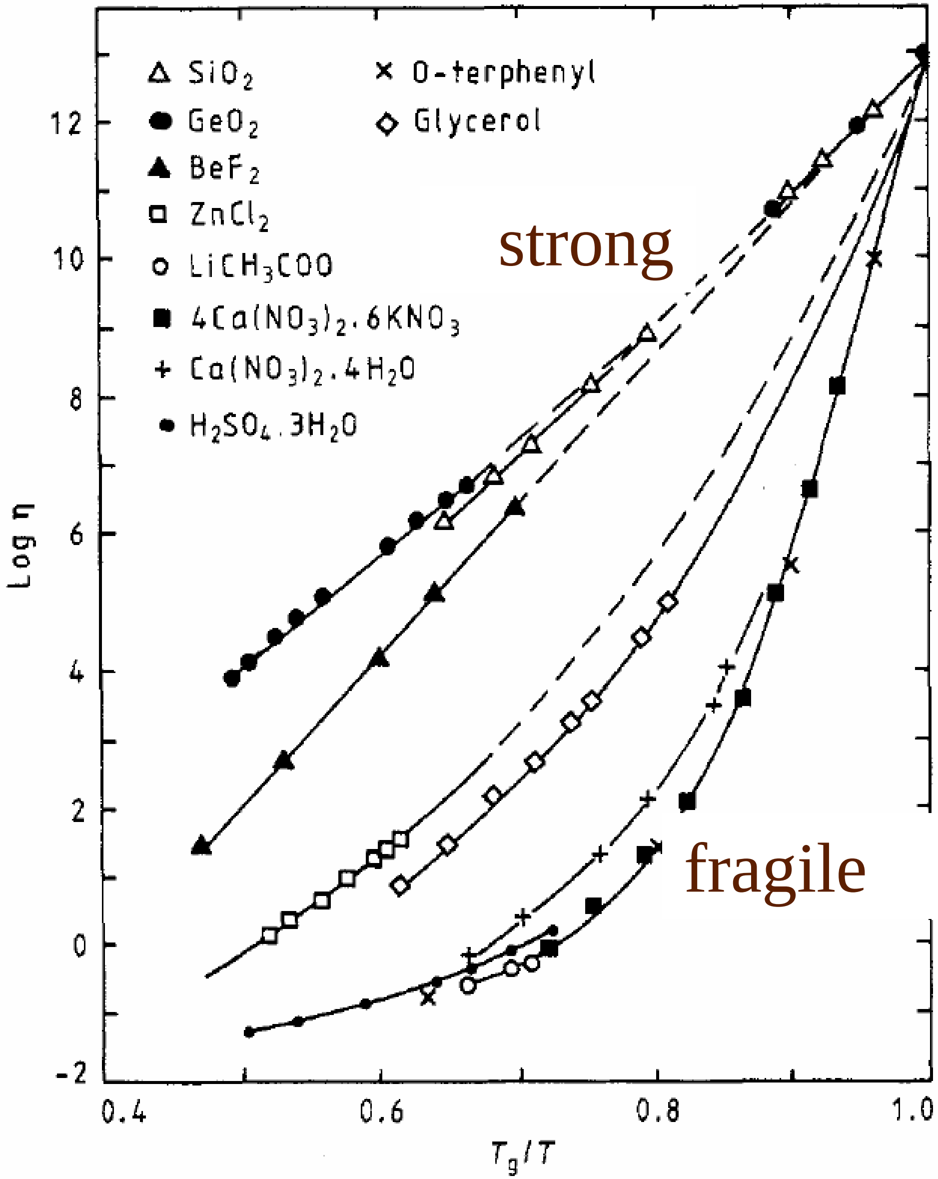

$$\eta = \exp\left(-\frac{E_0}{k(T-T_0)}\right)$$

VFT law

transition temperature T_0

Very strong variation of η / τ with temperature

T_g determined by state of the experimental technique

Differential Scanning Calorimetry (DSC)

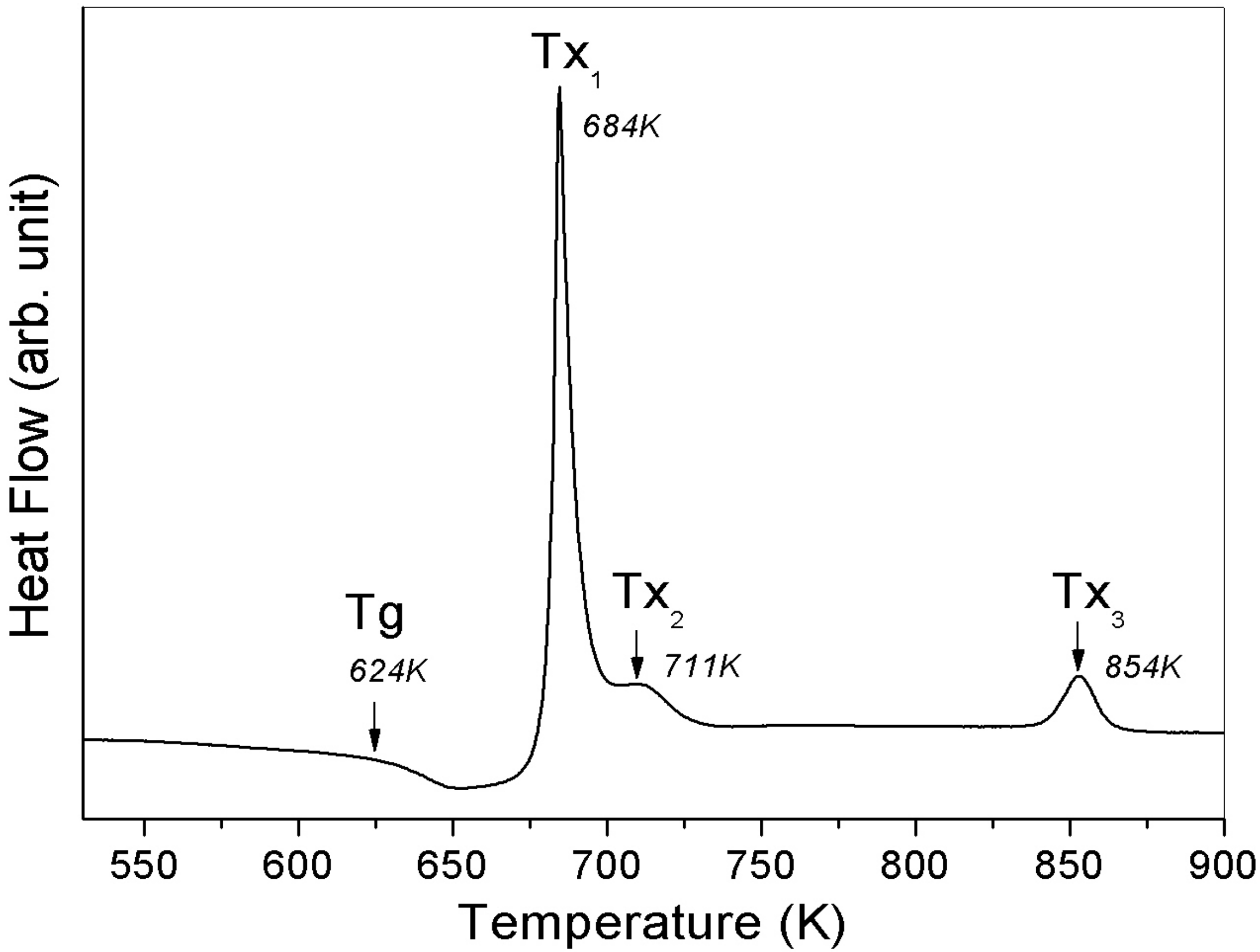

Differential Scanning Calorimetry

Supercooled liquid region:

$$\Delta T = T_{onsetx} - T_g$$

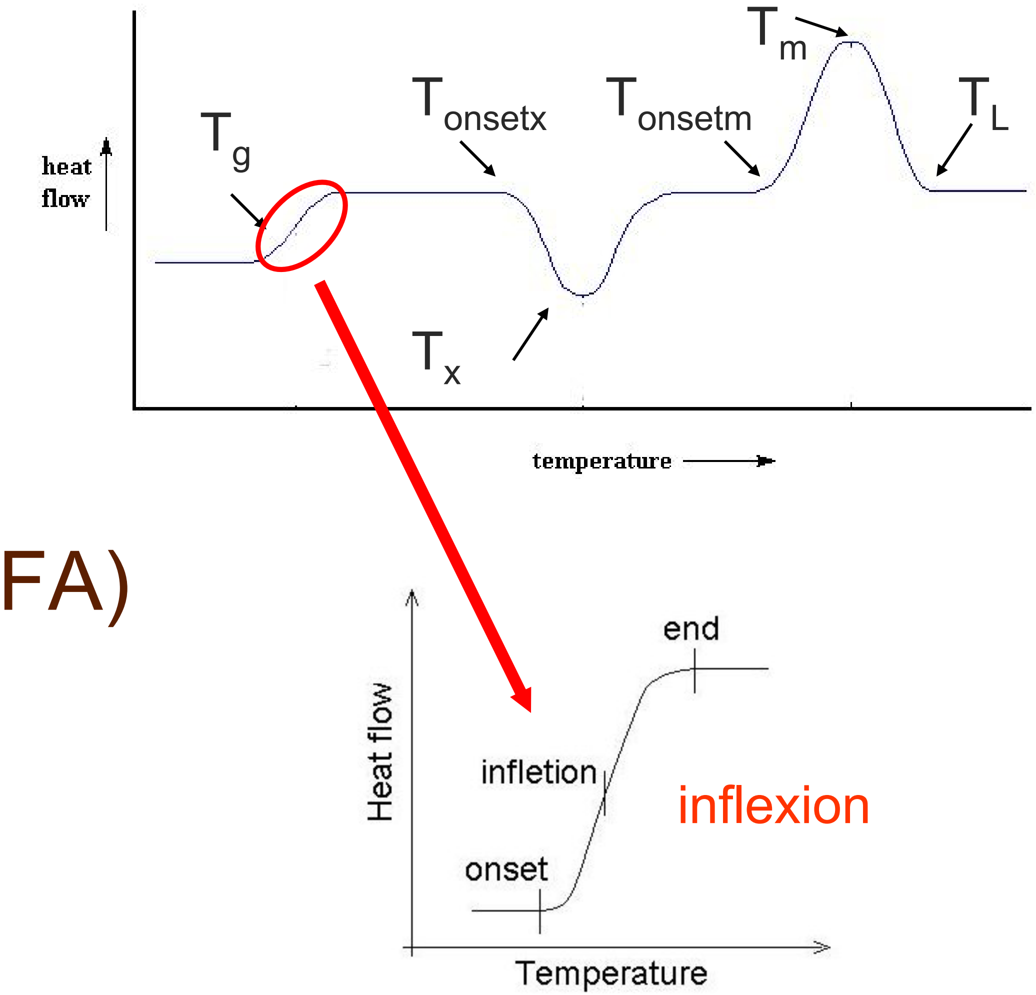

Glass forming ability (GFA)

$$\Delta T$$

$$T_{rg} = T_g / T_m$$

and many others

Kautzmann paradoxon

Glass transition at T_K when entropy of the amorphous is lower than in the corresponding crystal

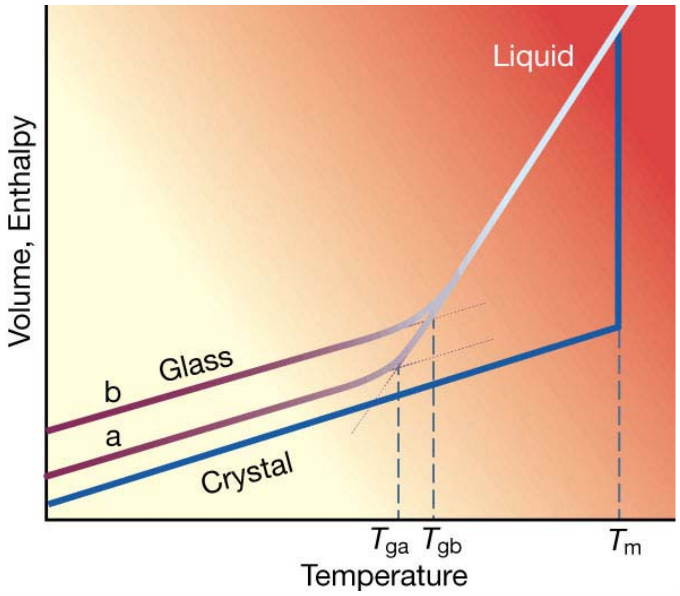

All real systems fall out of equilibrium before

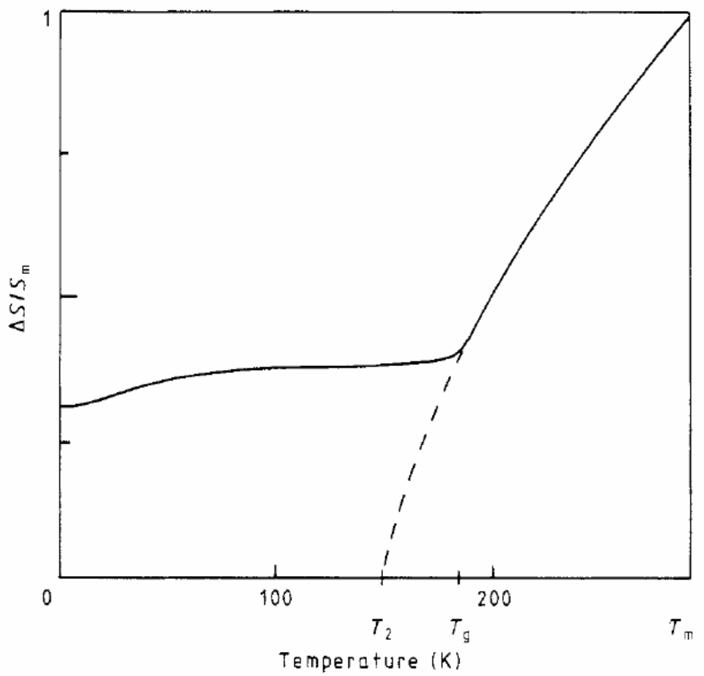

Glass transition

Dynamics in real disordered solids

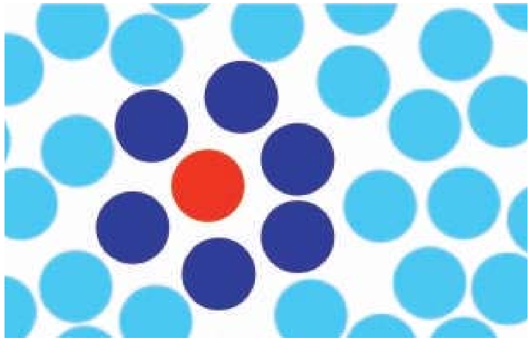

- microscopic process: rather harmonic in most glasses

- cage (β)- process: intermediate times

α- process: long range diffusion,
very strong T-dependence,
stretched exponential
$f_q \exp(-(t/\tau)^{\beta})$

glass transition T_c: α and β process merge

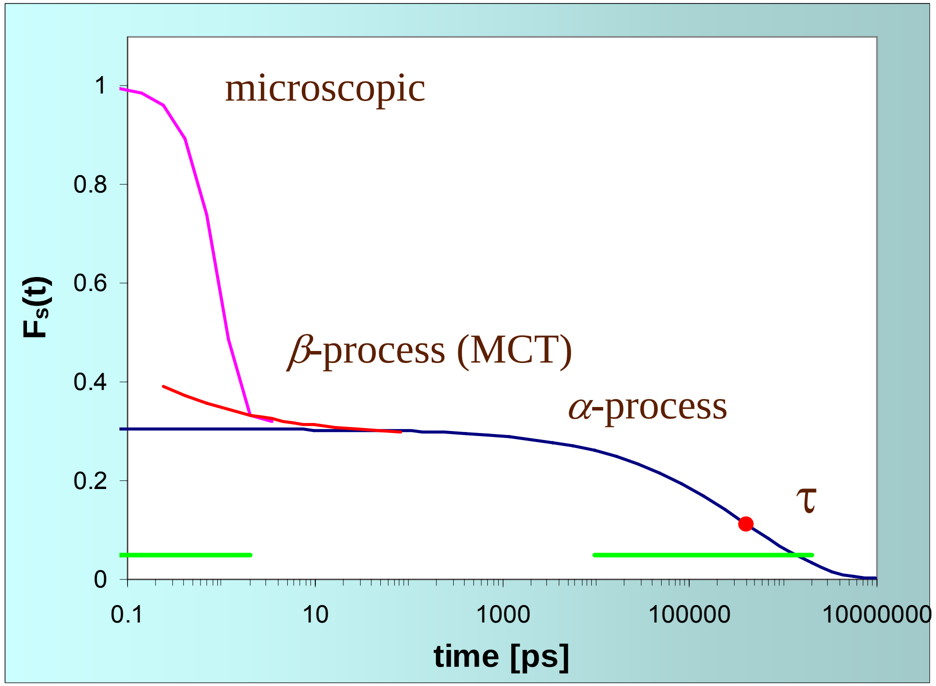

Density correlation functions and MCT

$$\phi_q(t) = \left\langle \rho_q^*(t)\rho_q(0)\right\rangle / \left\langle \left|\rho_q(0)\right|^2 \right\rangle$$

$$\ddot{\phi}_q(t) + \Omega_q^2 \phi_q(t) + \Omega_q^2 \int m_q(t-t')\dot{\phi}_q(t')dt' = 0$$

Equation of motion for density correlators including „memory term“

- Ergodicity - non-ergodicity transition at T_c
- Power laws for correlation functions near T_c
- Order parameter is the ergodicity parameter f_q

$$F_q(t) = f_q - h_q(t/\tau)^b + ... \approx f_q \exp(-t/\tau_K)^\beta$$

α-relaxation

$$F_q(t) = f_q + h_q(t_0/t)^a + ...$$

β-relaxation (cage process)

$$f_q \approx \sqrt{T_c - T}$$

Square-root singularity

Density correlation functions and MCT

$$f_q \approx \sqrt{T_c - T}$$

Square-root singularity

T_c describes a transition temperature which in contrast to T_g does not depend on experimental parameters.

The glass transition is an ergodic - non ergodic cross over

In most systems T_c is 20% higher than T_g, i.e. the transition is in the “liquid” region

The glass transition temperature T_g and T_c

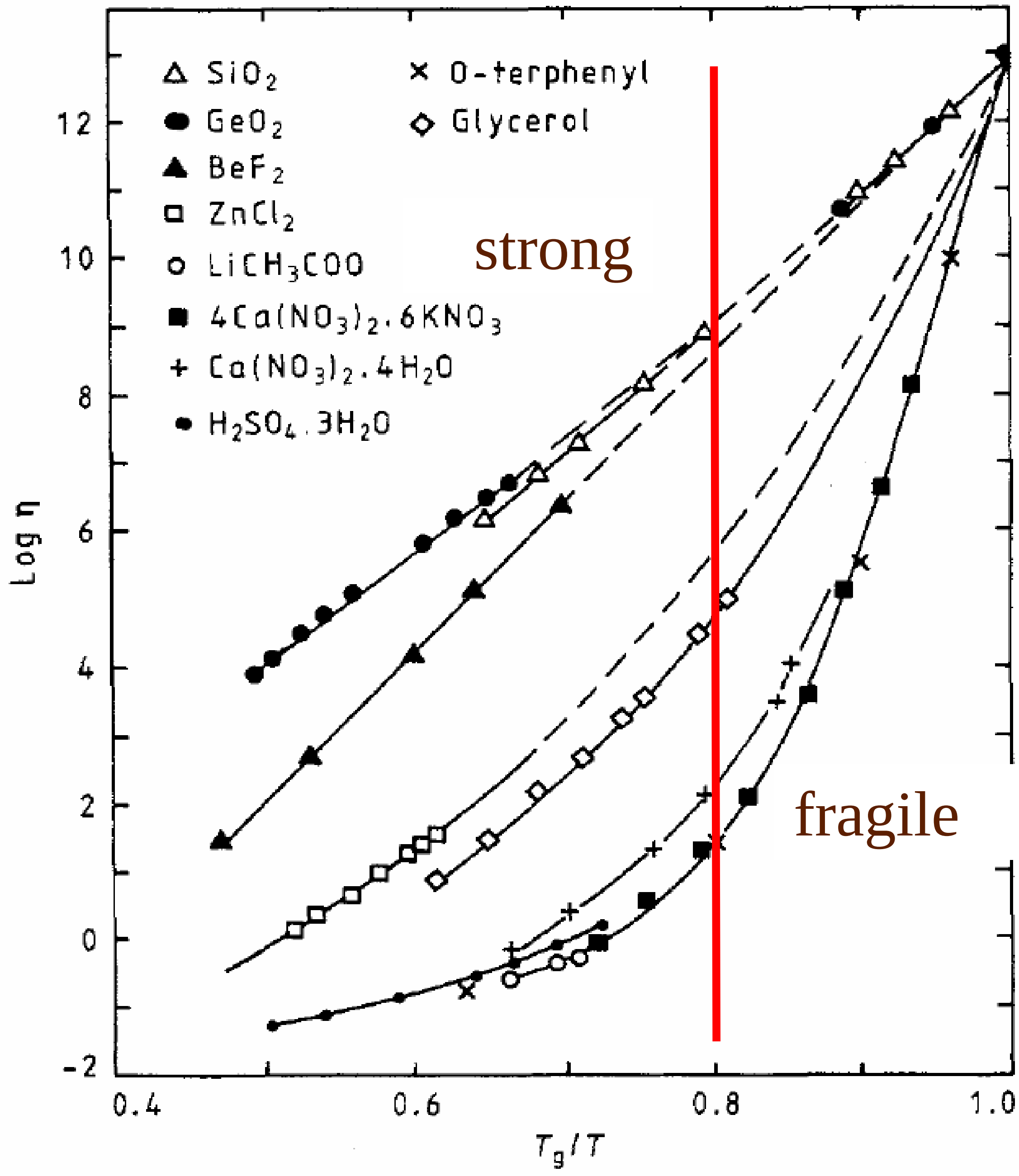

Density correlation functions and MCT

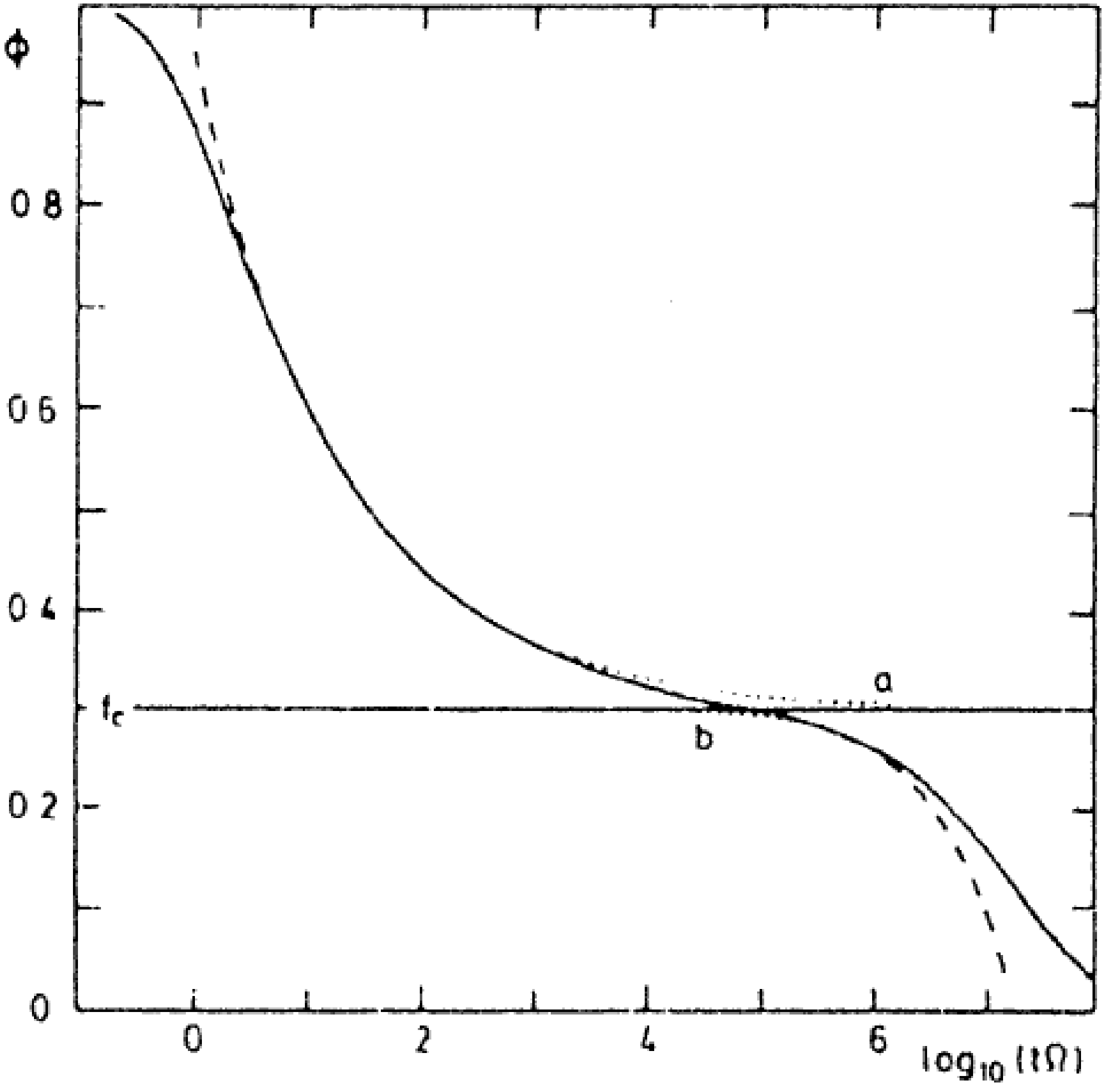

Figure 4. Comparison of the MCT solution for $\phi_q(t)$ (solid curve) with the asymptotic β-relaxation approximation (dashed curve) (equations (25) and (26)). The dotted curves show the two power laws. (From reference [4].)

MCT results for correlation functions at the glass transition

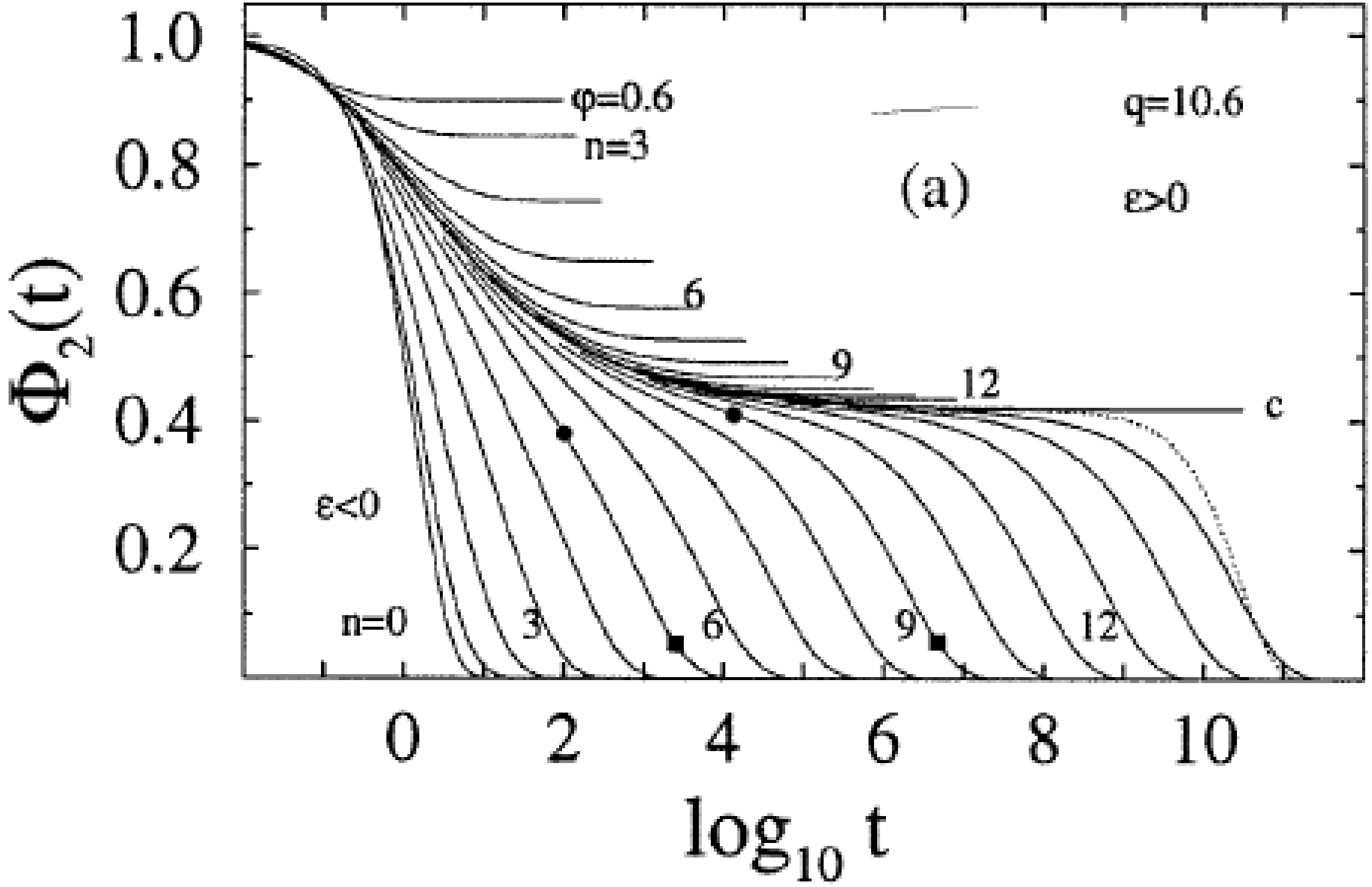

Nuclear resonant scattering

50 ps pulse,
tuned to the
transition
energy
$\Delta E \approx$ meV

$E = 14412.497$ eV,
$\Delta E = 4.7$ neV

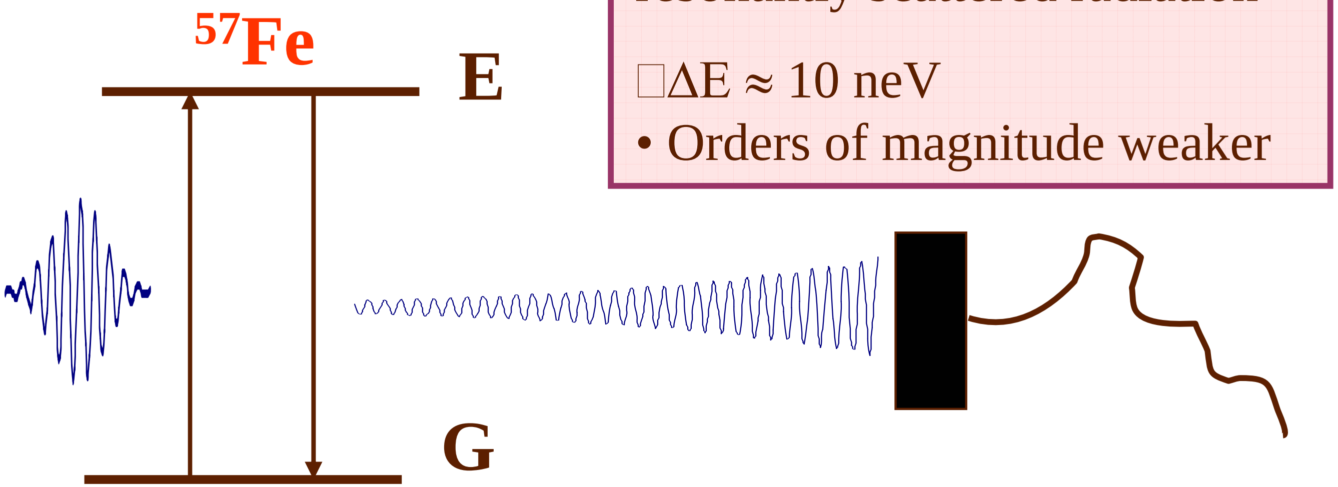

Transmitted pulse, plus resonantly scattered radiation

□$\Delta E \approx 10$ neV

- Orders of magnitude weaker

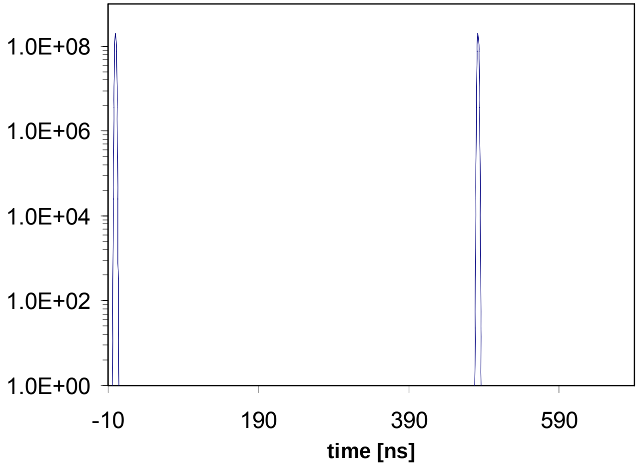

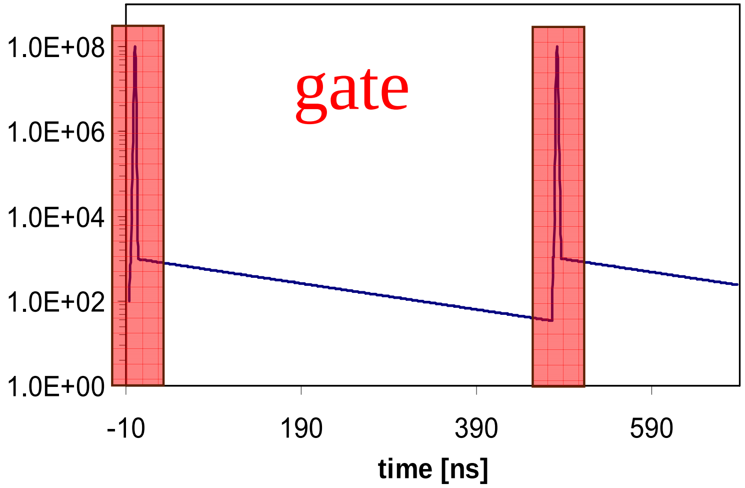

NRS set-up

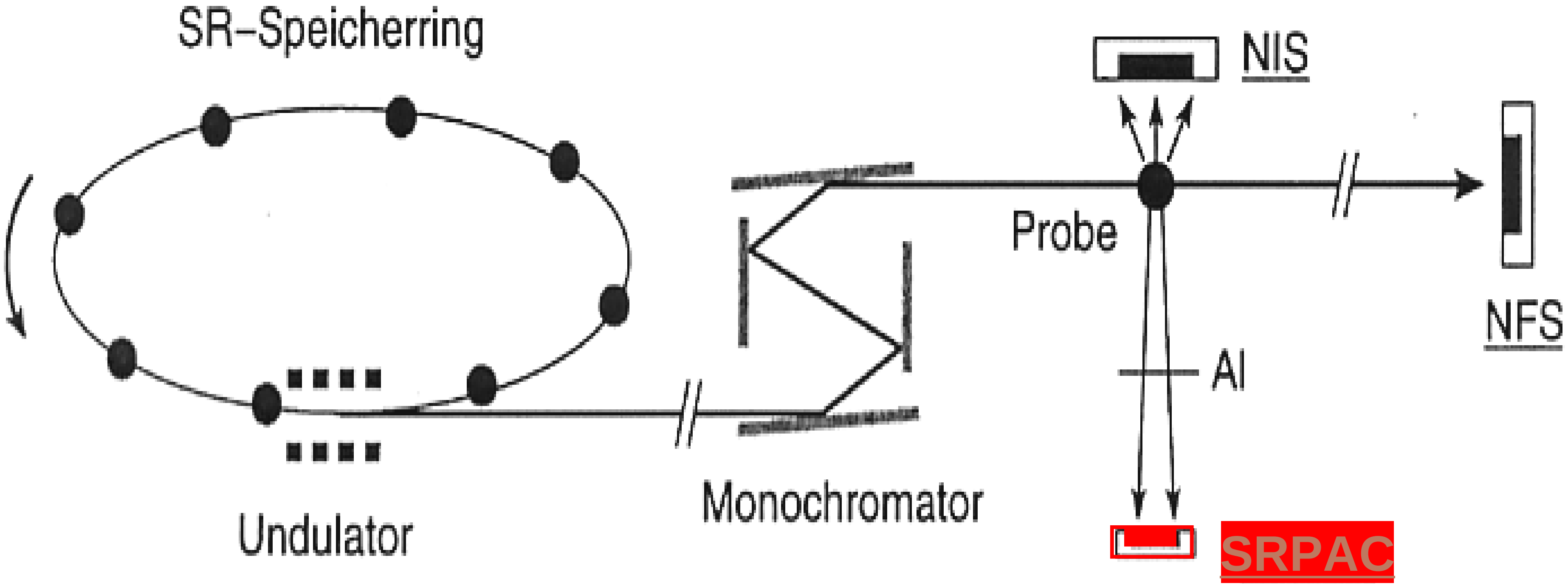
SR–Speicherring
NIS
Probe
NFS
Al
Undulator
Monochromator
SRPAC

Quasielastic nuclear resonant forward scattering

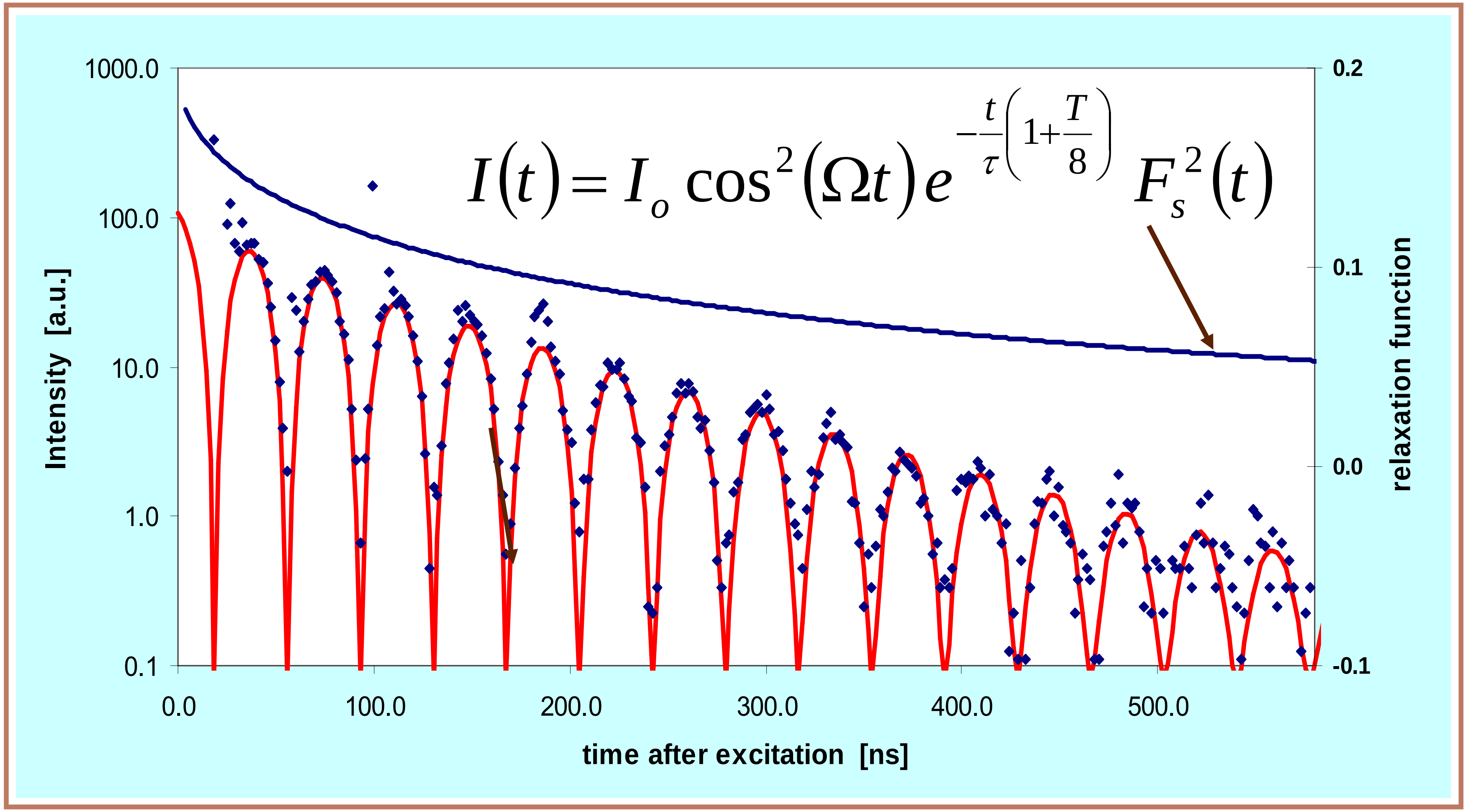

$$I(t) = I_o \cos^2(\Omega t)\, e^{-\frac{t}{\tau}\left(1+\frac{T}{8}\right)}\, F_s^{\,2}(t)$$

Butyl phthalate / ferrocene

Exact treatment of QNFS: I. Sergueev, HF,.. PRB 2003

Non ergodicity parameter

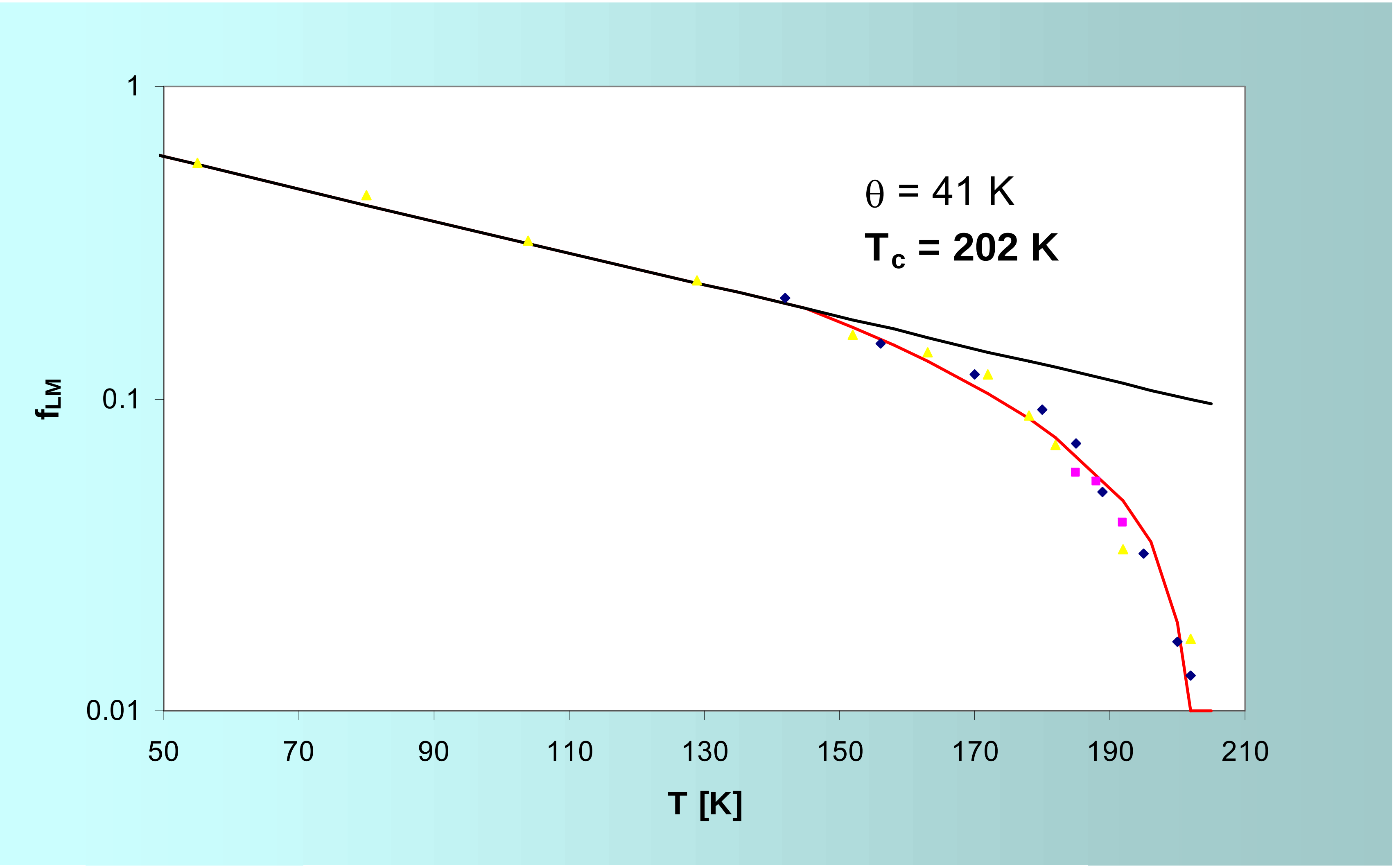

Square-root behaviour as predicted by mode-coupling theory

Stretching exponent $\beta = 0.48$, independent of T

Relaxation rates

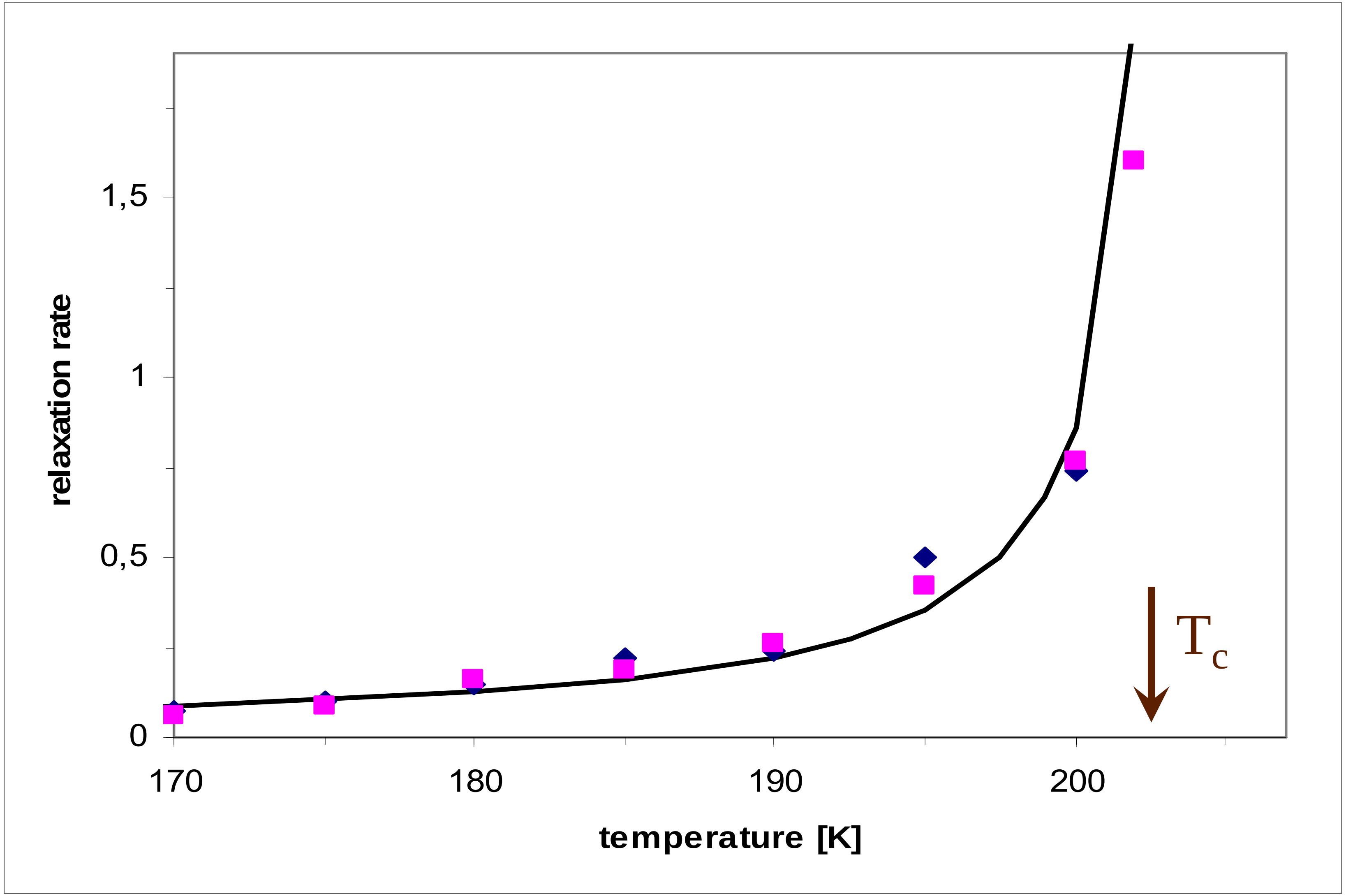

T. Asthalter, I.Sergueev, HF, et al EPJ B (2001)

Neutron scattering results

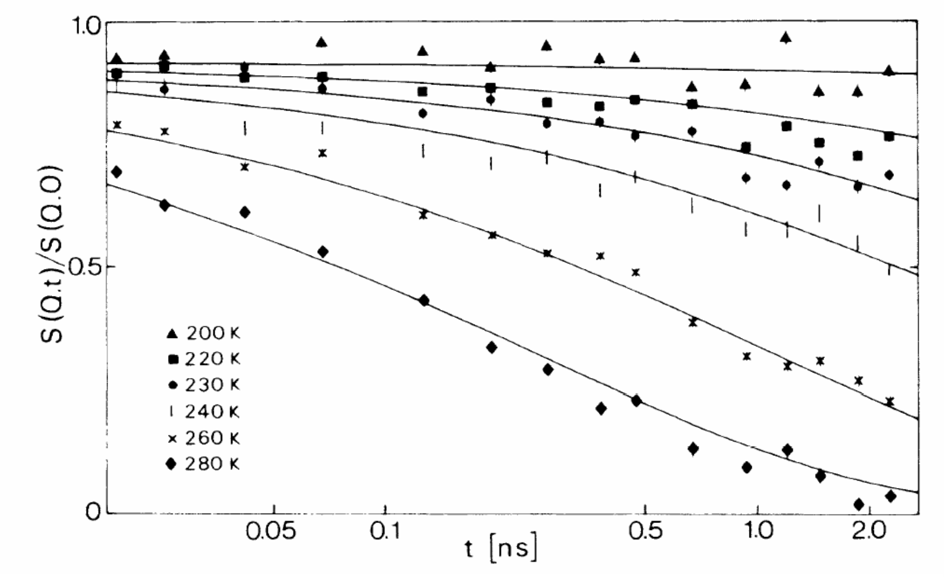

Masterplot

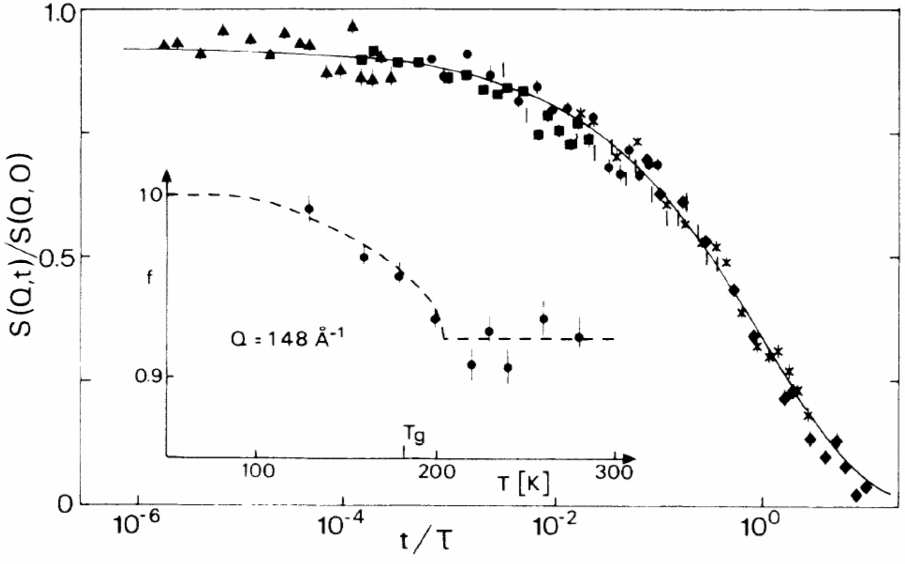

J. Wuttke et al, Physica B (1997)

Dielectric spectroscopy

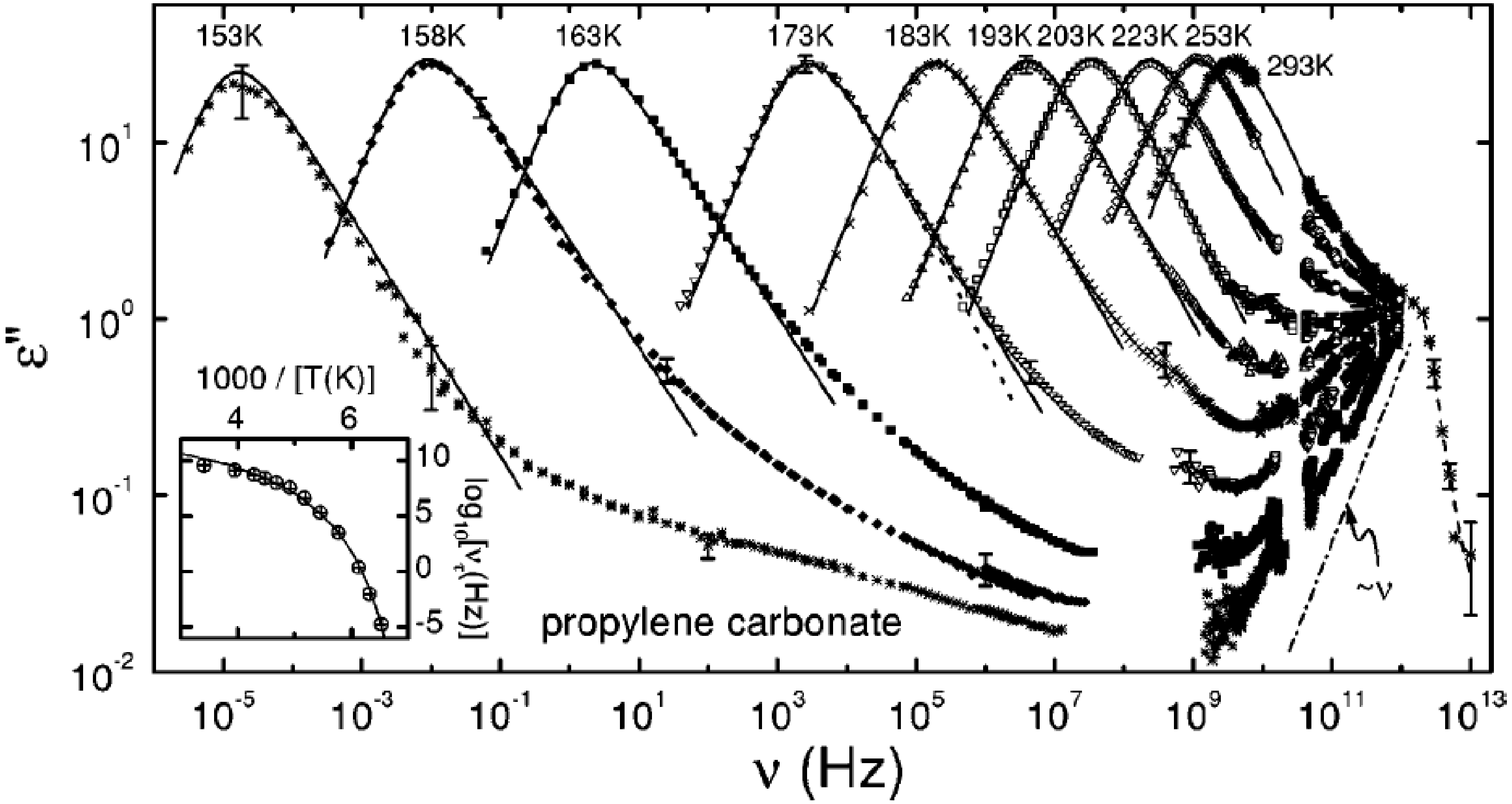

FIG. 2. Frequency dependence of the dielectric loss in propylene carbonate at various temperatures. The solid lines are fits with the CD function, the dotted line is a fit with the Fourier transform of the KWW law, both performed simultaneously on ε'. The dash-dotted line indicates a linear increase. The FIR results have been connected by a dashed line to guide the eye. The inset shows $\nu_\tau = 1/(2\pi\langle\tau\rangle)$ as resulting from the CD (circles) and KWW fits (pluses) in an Arrhenius representation. The line is a fit using the VFT expression, Eq. (1), with $T_{VF} = 132$ K, $D = 6.6$, and $\nu_0 = 3.2 \times 10^{12}$ Hz.

U. Schneider et al. PRE (1999)

Bulk Metallic Glasses

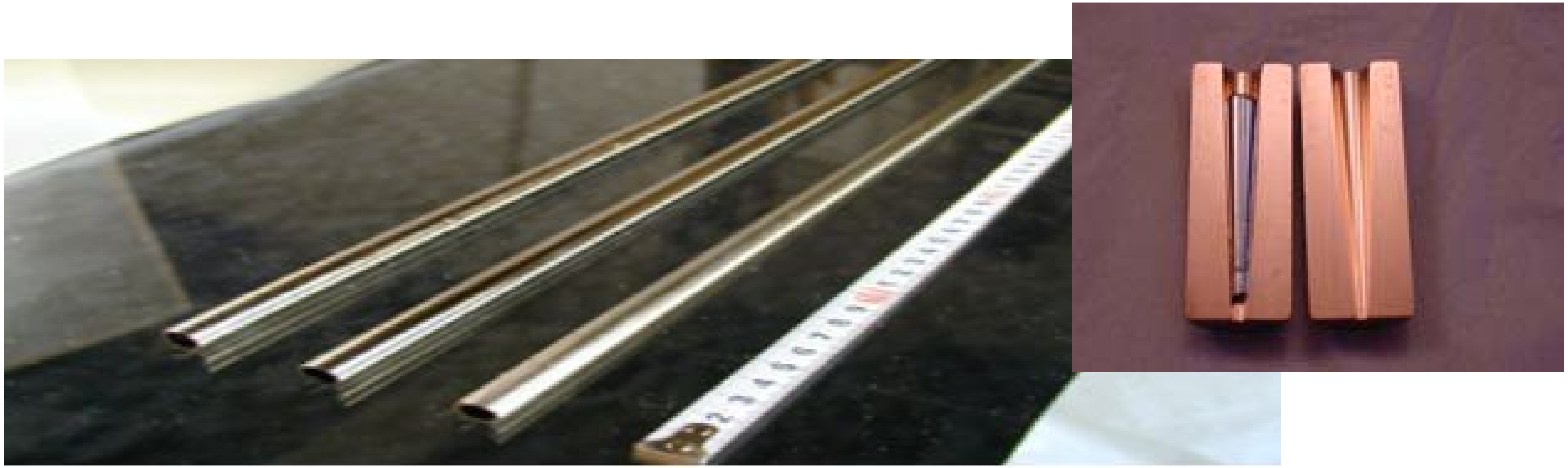

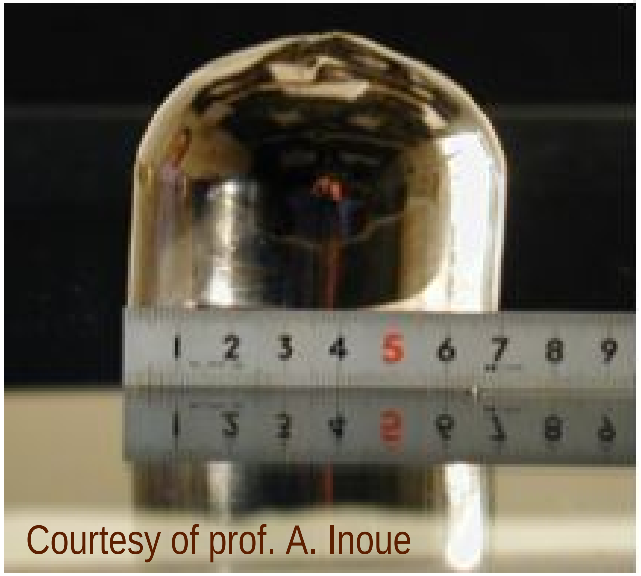
Courtesy of prof. A. Inoue

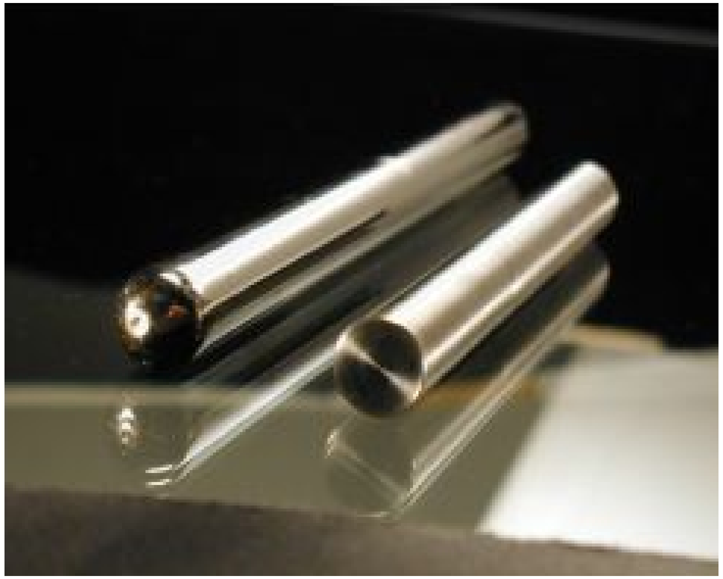

Systems

- Historically first alloy AuSi (1960) cooling with 10^6 K/s
- 1969 PdCuSi – only 10^3 K/s needed
- First commercial amorphous alloy, Vitreloy 1 (41.2% Zr, 13.8% Ti, 12.5% Cu, 10% Ni, 22.5% Be)
- Families of alloys
  - Pd based: PdCuNiP
  - Zr based: ZrNi, ZrTiCuNiBe (v4), ZrAlNiCuAg, ZrPd, ZrAlCu, ZrAlCuNiFe
  - La based
  - Fe based: FePCAlBGa
  - Cu based: CuZr, CuTiZr
  - Al based: AlLaNi
  - Ni based: NiZr, NiNbY

  - and many more

Systems

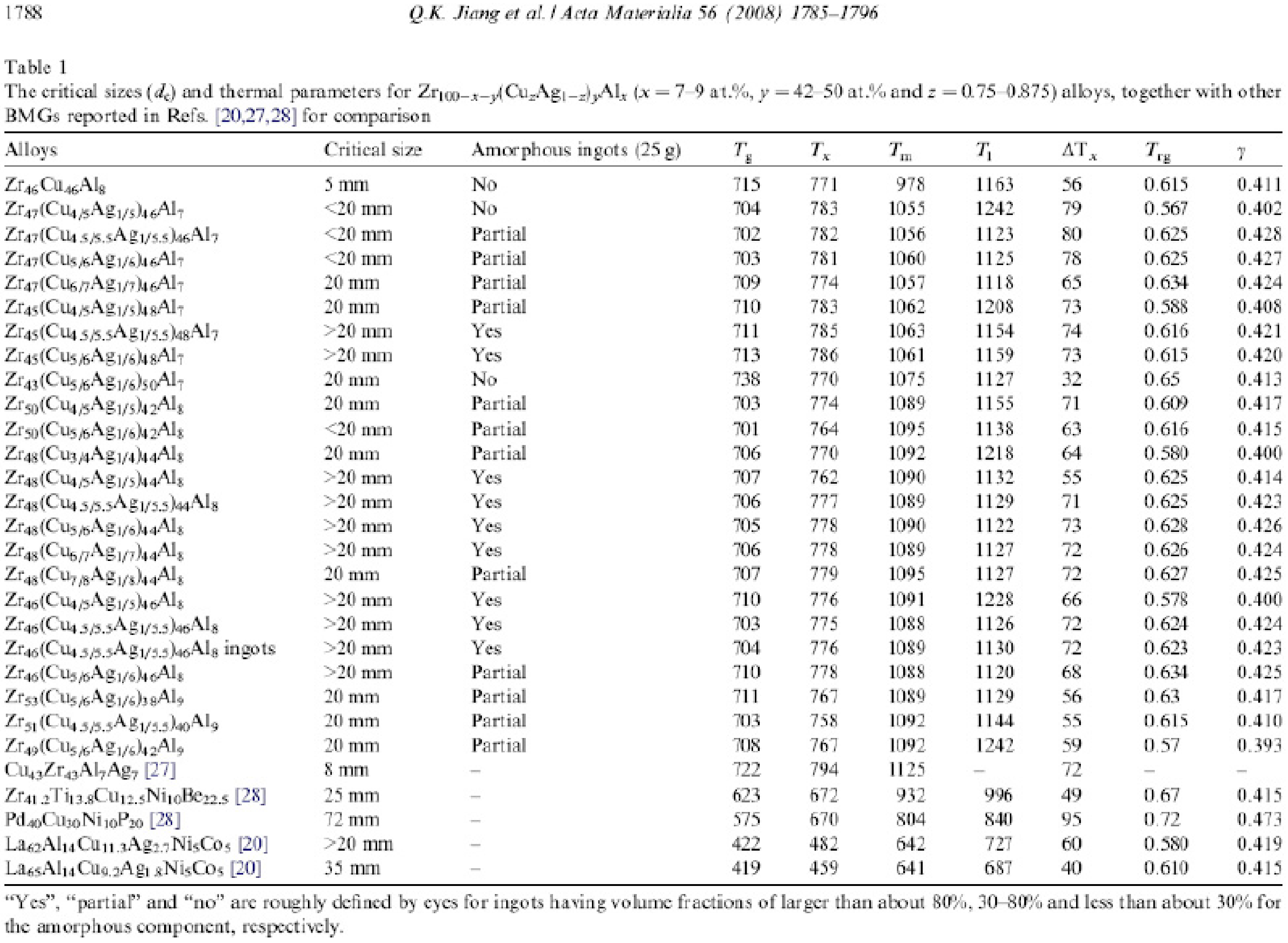

1788 *Q.K. Jiang et al. / Acta Materialia 56 (2008) 1785–1796*

Table 1
The critical sizes (d_c) and thermal parameters for $Zr_{100-x-y}(Cu_zAg_{1-z})_yAl_x$ ($x = 7$–9 at.%, $y = 42$–50 at.% and $z = 0.75$–0.875) alloys, together with other BMGs reported in Refs. [20,27,28] for comparison

Alloys	Critical size	Amorphous ingots (25 g)	T_g	T_x	T_m	T_l	ΔT_x	T_{rg}	γ
$Zr_{46}Cu_{46}Al_8$	5 mm	No	715	771	978	1163	56	0.615	0.411
$Zr_{47}(Cu_{4/5}Ag_{1/5})_{46}Al_7$	<20 mm	No	704	783	1055	1242	79	0.567	0.402
$Zr_{47}(Cu_{4.5/5.5}Ag_{1/5.5})_{46}Al_7$	<20 mm	Partial	702	782	1056	1123	80	0.625	0.428
$Zr_{47}(Cu_{5/6}Ag_{1/6})_{46}Al_7$	<20 mm	Partial	703	781	1060	1125	78	0.625	0.427
$Zr_{47}(Cu_{6/7}Ag_{1/7})_{46}Al_7$	20 mm	Partial	709	774	1057	1118	65	0.634	0.424
$Zr_{45}(Cu_{4/5}Ag_{1/5})_{48}Al_7$	20 mm	Partial	710	783	1062	1208	73	0.588	0.408
$Zr_{45}(Cu_{4.5/5.5}Ag_{1/5.5})_{48}Al_7$	>20 mm	Yes	711	785	1063	1154	74	0.616	0.421
$Zr_{45}(Cu_{5/6}Ag_{1/6})_{48}Al_7$	>20 mm	Yes	713	786	1061	1159	73	0.615	0.420
$Zr_{43}(Cu_{5/6}Ag_{1/6})_{50}Al_7$	20 mm	No	738	770	1075	1127	32	0.65	0.413
$Zr_{50}(Cu_{4/5}Ag_{1/5})_{42}Al_8$	20 mm	Partial	703	774	1089	1155	71	0.609	0.417
$Zr_{50}(Cu_{5/6}Ag_{1/6})_{42}Al_8$	<20 mm	Partial	701	764	1095	1138	63	0.616	0.415
$Zr_{48}(Cu_{3/4}Ag_{1/4})_{44}Al_8$	20 mm	Partial	706	770	1092	1218	64	0.580	0.400
$Zr_{48}(Cu_{4/5}Ag_{1/5})_{44}Al_8$	>20 mm	Yes	707	762	1090	1132	55	0.625	0.414
$Zr_{48}(Cu_{4.5/5.5}Ag_{1/5.5})_{44}Al_8$	>20 mm	Yes	706	777	1089	1129	71	0.625	0.423
$Zr_{48}(Cu_{5/6}Ag_{1/6})_{44}Al_8$	>20 mm	Yes	705	778	1090	1122	73	0.628	0.426
$Zr_{48}(Cu_{6/7}Ag_{1/7})_{44}Al_8$	>20 mm	Yes	706	778	1089	1127	72	0.626	0.424
$Zr_{48}(Cu_{7/8}Ag_{1/8})_{44}Al_8$	20 mm	Partial	707	779	1095	1127	72	0.627	0.425
$Zr_{46}(Cu_{4/5}Ag_{1/5})_{46}Al_8$	>20 mm	Yes	710	776	1091	1228	66	0.578	0.400
$Zr_{46}(Cu_{4.5/5.5}Ag_{1/5.5})_{46}Al_8$	>20 mm	Yes	703	775	1088	1126	72	0.624	0.424
$Zr_{46}(Cu_{4.5/5.5}Ag_{1/5.5})_{46}Al_8$ ingots	>20 mm	Yes	704	776	1089	1130	72	0.623	0.423
$Zr_{46}(Cu_{5/6}Ag_{1/6})_{46}Al_8$	>20 mm	Partial	710	778	1088	1120	68	0.634	0.425
$Zr_{53}(Cu_{5/6}Ag_{1/6})_{38}Al_9$	20 mm	Partial	711	767	1089	1129	56	0.63	0.417
$Zr_{51}(Cu_{4.5/5.5}Ag_{1/5.5})_{40}Al_9$	20 mm	Partial	703	758	1092	1144	55	0.615	0.410
$Zr_{49}(Cu_{5/6}Ag_{1/6})_{42}Al_9$	20 mm	Partial	708	767	1092	1242	59	0.57	0.393
$Cu_{43}Zr_{43}Al_7Ag_7$ [27]	8 mm	–	722	794	1125	–	72	–	–
$Zr_{41.2}Ti_{13.8}Cu_{12.5}Ni_{10}Be_{22.5}$ [28]	25 mm	–	623	672	932	996	49	0.67	0.415
$Pd_{40}Cu_{30}Ni_{10}P_{20}$ [28]	72 mm	–	575	670	804	840	95	0.72	0.473
$La_{62}Al_{14}Cu_{11.3}Ag_{2.7}Ni_5Co_5$ [20]	>20 mm	–	422	482	642	727	60	0.580	0.419
$La_{65}Al_{14}Cu_{9.2}Ag_{1.8}Ni_5Co_5$ [20]	35 mm	–	419	459	641	687	40	0.610	0.415

"Yes", "partial" and "no" are roughly defined by eyes for ingots having volume fractions of larger than about 80%, 30–80% and less than about 30% for the amorphous component, respectively.

Favorable conditions for glass formation

Couple of empirical rules in literature

However up to now still empirical (trail and error) development

- **Three or more alloy components**
- **Very different atomic radii**
- **Negative heat of mixing**
- **Low eutectic**
- **Competing crystalline phases**

Structure vs. macroscopic properties

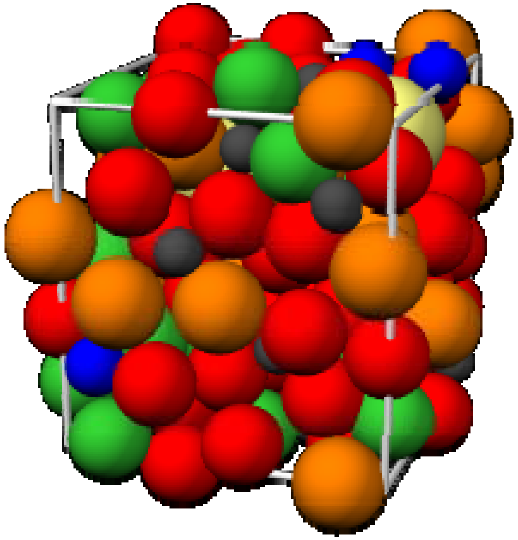

Understanding relation between the structure and macroscopic properties is important for improving performance of existing and crucial for designing novel materials